Received: 4 May 2024 | Revised: 22 July 2024 | Accepted: 10 August 2024

DOI: 10.1002/arch.22146

RESEARCH ARTICLE

Archives of INSECT BIOCHEMISTRY AND PHYSIOLOGY WILEY

Exploring the role of RNASET2 in the immune response of black soldier fly larvae

Sara Caramella[1] | Nicolò Baranzini[1] | Daniele Bruno[1] | Viviana Teresa Orlandi[1] | Amr Mohamed[2,3] | Fabrizio Bolognese[1] | Annalisa Grimaldi[1] | Gianluca Tettamanti[1,4]

[1]Department of Biotechnology and Life Sciences, University of Insubria, Varese, Italy

[2]Department of Entomology, Faculty of Science, Cairo University, Giza, Egypt

[3]Plant Protection Department, College of Food and Agricultural Sciences, King Saud University Museum of Arthropods, King Saud University, Riyadh, Saudi Arabia

[4]Interuniversity Center for Studies on Bioinspired Agro-Environmental Technology (BAT Center), University of Napoli Federico II, Napoli, Italy

Correspondence

Daniele Bruno, Department of Biotechnology and Life Sciences, University of Insubria, Varese, Italy.
Email: daniele.bruno@uninsubria.it

Funding information

Ministero dell'Istruzione, dell'Università e della Ricerca - Finanziamento dell'Unione Europea - NextGenerationEU - PNRR Missione 4, Componente 2, Investimento 1.1, Grant/Award Number: PRIN-PNRR 2022 - grant n° P2022MZAF8

Abstract

T2 RNases are transferase-type enzymes distributed across phyla, crucial for breaking down single-stranded RNA molecules. In addition to their canonical function, several T2 enzymes exhibit pleiotropic roles, contributing to various biological processes, such as the immune response in invertebrates and vertebrates. This study aims at characterizing RNASET2 in the larvae of black soldier fly (BSF), *Hermetia illucens*, which are used for organic waste reduction and the production of valuable insect biomolecules for feed formulation and other applications. Given the exposure of BSF larvae to pathogens present in the feeding substrate, it is likely that the mechanisms of their immune response have undergone significant evolution and increased complexity. After in silico characterization of HiRNASET2, demonstrating the high conservation of this T2 homolog, we investigated the expression pattern of the enzyme in the fat body and hemocytes, two districts mainly involved in the insect immune response, in larvae challenged with bacterial infection. While no variation in HiRNASET2 expression was observed in the fat body following infection, a significant upregulation of HiRNASET2

Sara Caramella and Nicolò Baranzini contributed equally to this study.

synthesis occurred in hemocytes shortly after the injection of bacteria in the larva. The intracellular localization of HiRNASET2 in lysosomes of plasmatocytes, its extracellular association with bacteria, and the presence of a putative antimicrobial domain in the molecule, suggest its potential role in RNA clean-up and as an alarm molecule promoting phagocytosis activation by hemocytes. These insights contribute to the characterization of the immune response of *Hermetia illucens* larvae and may facilitate the development of animal feedstuff enriched with highly valuable BSF bioactive compounds.

KEYWORDS

bacterial infection, fat body, hemocytes, immune response, T2 RNases

Research Highlights

- In silico analysis demonstrated the presence of a conserved RNASET2 homolog in *Hermetia illucens* larvae
- An upregulation of HiRNASET2 synthesis in plasmatocytes occurred after bacterial infection
- A putative peptide with antimicrobial activity was identified in HiRNASET2

1 | INTRODUCTION

Transferase-type ribonucleases, also known as RNases, are a wide class of enzymes that catalyze the hydrolysis of single-stranded RNA molecules through the formation of a cyclic transient intermediate, which results in the production of 3′-phosphate mononucleotides (MacIntosh et al., 2001). Despite this unique mechanism of action, due to their different biochemical characteristics, these proteins have been divided into A, T1, and T2 families (Deshpande & Shankar, 2002), of which T2 is the only one widely spread throughout the tree of life and beyond. In fact, it has been identified from viruses to eukaryotes (Nicholson, 2011; Pizzo & D'Alessio, 2007), where it shows a pleiotropic role carrying out diverse biological functions in different organisms (Luhtala & Parker, 2010; MacIntosh, 2011). Purified and characterized for the first time from *Aspergillus oryziae* and *Rhizopus niveus* enzyme extracts (Horiuchi et al., 1988; Kawata et al., 1988; Sato & Egami, 1957), all the T2 RNases show a conserved three-dimensional structure, composed of a core of six α-helices and seven β-strands (De & Funatsu, 1992; Inokuchi et al., 1993; Kobayashi et al., 1992), in which two conserved active sites (CASI and CASII), involved in the main catalytic activity, are present (Irie, 1999; Kawata et al., 1990; Kurihara et al., 1992). The major turning point in the functional investigations of these molecules was attributed to McClure et al. (1989) who not only observed an elevated degree of homology between fungal and plant T2 RNases but also demonstrated that the latter were involved in self-incompatibility processes showing, for the first time, unexpected evidence related to alternative biological roles of T2 enzymes (Deshpande & Shankar, 2002). From here, the exploration of additional traits and biological attributes about these enzymes has intensified the debate within the scientific community. The heightened interest toward these RNases is further promoted by the observation that diverse functions are frequently linked to specific

intracellular and extracellular locations. Indeed, several RNases have been found in diverse subcellular compartments, such as vacuoles and lysosomes, or in the extracellular environment (Baranzini et al., 2019; Campomenosi et al., 2006; MacIntosh, 2011), where RNA molecules are not typically present, highlighting the possible loss of the catalytic activity and the acquisition of atypical specializations (MacIntosh, 2011).

A single *RNASET2* gene, encoding three different isoforms, was found in the human genome. The isoform with the highest molecular weight is secreted in the extracellular environment (Campomenosi et al., 2006), playing a pivotal role in the regulation of immune response (Acquati et al., 2011). Moreover, some T2 RNase homologs play a crucial role in the regulation of the innate immune response in invertebrates, such as the Mediterranean mussel *Mytilus galloprovincialis* (Parisi et al., 2022) and the leech *Hirudo verbana* (Annelida, Hirudinea) (Baranzini et al., 2020a), by recruiting phagocytic cells for a rapid and effective eradication of potential pathogens. Furthermore, it has been shown that these enzymes may play a crucial role not only in the inflammatory response, but also in wound healing processes. Indeed, HvRNASET2 injection into the leech body wall induces massive collagen production and rapid connective tissue remodeling (Baranzini et al., 2021), mimicking the wound healing process (Tettamanti et al., 2003; Tettamanti et al., 2003).

In addition, in leeches HvRNASET2 possesses a putative antibacterial motif that seems to act against both Gram-positive and Gram-negative bacteria, affecting cell membranes and reducing their viability (Baranzini et al., 2020b). T2 RNases have been identified in insects, too, but playing different biological functions. Indeed, in the saliva and salivary glands of the plant bugs *Halyomorpha halys* and *Nezara viridula*, a transcriptomic analysis showed a high expression of Oy-like RNase, belonging to the T2 RNase family, whose role seems to be associated with plant RNA degradation during extra-oral digestion (Castellanos et al., 2017; Liu & Bonning, 2019; Liu et al., 2018). In *Drosophila melanogaster*, a T2 ribonuclease homolog known as RNase X25 is active during every stage of development, performing a housekeeping function to maintain cellular homeostasis, but also playing an essential role in the response to starvation (Ambrosio et al., 2014). In addition, since the humoral immune response in the lepidopteran *Galleria mellonella* is activated by exogenous RNASET2 enzymes secreted by the pathogenic fungus *Beauveria bassiana* (Yue et al., 2023), we can speculate that, even in insects, endogenous RNASET2 may have a conserved role in modulating the immune response.

Here we propose the larvae of the black soldier fly (BSF), *Hermetia illucens* (Diptera: Stratiomyidae), as a model to elucidate the possible role of RNASET2 in the activation and modulation of the insect immune system. In fact, the exposure to high bacterial concentrations in the decaying substrates where these larvae grow likely led to the evolution of a sophisticated immune system that can efficiently counteract infections. Since in these larvae an articulated, finely tuned immune response takes place following bacterial challenge (Bruno et al., 2021, 2023; Zdybicka-Barabas et al., 2017), we undertook the identification of a RNASET2 homolog in this dipteran and explored the potential role of such a versatile molecule in the regulation of BSF immunity. In detail, after in silico analysis of HiRNASET2, its expression and localization were assessed in larvae infected with *Micrococcus luteus* and *Escherichia coli*. In addition, the antimicrobial activity of HiRNASET2 was addressed through in vitro analyses.

Comprehending the physiology of *H. illucens*, particularly delving into regulatory mechanisms that underpin its immune response, not only expands knowledge of the defense processes in Diptera, but also holds significant importance for optimizing mass rearing of BSF in production plants and obtain microbiologically safe larvae for different purposes (Ceccotti et al., 2022; Mannucci et al., 2024). In fact, the implementation of BSF-based feedstuff with antimicrobial molecules could lead to a reduced use of antibiotics in farming procedures and, at the same time, determine an improved health status of livestock.

2 | MATERIALS AND METHODS

2.1 | In silico analysis of HiRNASET2

HiRNASET2 amino acid sequence (Protein ID: XP_037927009.1) was obtained from the National Center for Biotechnology Information (https://www.ncbi.nlm.nih.gov). The molecular weight was calculated by ExPASy Compute

pI/Mw Tool (https://web.expasy.org/compute_pi/); both amino acid length and active sites were determined using PROSITE (https://prosite.expasy.org/scanprosite/).

The primary structure of HiRNASET2 was compared with that of *Tribolium castaneum* (XP_975968.1), *Sitophilus oryzae* (XP_030752536.1), *Cimex lectularius* (XP_014255552.1), *Bombyx mori* (XP_004929436.1), *Anopheles aquasalis* (XP_050085435.1), *Drosophila biarmipes* (XP_016966519.1), *Bombus affinis* (XP_050574557.1), *Vespula vulgaris* (XP_050858617.1), *Formica exsecta* (XP_029667733.1), *Trichinella spiralis* (KRY35497.1), *Clonorchis sinensis* (KAG5442322.1), *Daphnia magna* (XP_032782435.2), *Penaeus vannamei* (ROT65430.1), and *Crassostrea gigas* (XP_034325182.1) using Clustal Omega (https://www.ebi.ac.uk/Tools/msa/clustalo/) (Sievers et al., 2011) and the graphical output was created with Jalview (http://www.jalview.org/) (Waterhouse et al., 2009). The identification of functional regions was performed with ConSurf (https://consurf.tau.ac.il/) (Berezin et al., 2004). The three-dimensional structure was developed using I-TASSER (IterativeThreading ASSEmbly Refinement) modeling server (https://zhanglab.ccmb.med.umich.edu/I-TASSER/) (Zhang, 2008) starting from structural templates of homologous T2 enzymes obtained from the Protein Data Bank (PBD) library (https://www.rcsb.org/) (Berman et al., 2002). The resulting PDB file was visualized and analyzed with PyMOL software (https://pymol.org/2/) to define the secondary structure. QMEANDisCo analysis (https://swissmodel.expasy.org/qmean/) was performed to validate the accuracy of the obtained secondary structure.

To get insight into the functional role of HiRNASET2, the presence of a N-terminal signal peptide and the possible subcellular localization were predicted using SignalP-6.0 (http://www.cbs.dtu.dk/services/SignalP/) (Teufel et al., 2022) and DeepLoc 2.0 server (http://www.cbs.dtu.dk/services/TMHMM/) (Möller et al., 2001), respectively. In addition, the presence of putative antimicrobial peptides in the molecule was evaluated by AMPA (http://tcofee.crg.cat/apps/ampa/do) (Torrent et al., 2012).

2.2 | Insect rearing

BSF larvae were obtained from a colony established at University of Insubria and reared according to Pimentel et al. (2017). Briefly, 4 days after hatching, batches of 300 larvae were placed in 16 × 16 × 9 cm plastic containers and fed on standard diet for Diptera (Hogsette, 1992), modified to obtain 1,28 protein to carbohydrate (P:C) ratio, in which casein and starch were used as protein and carbohydrate source, respectively. In addition, cellulose was added as nonnutritive bulking agent to reach the desired P:C ratio. Larvae were reared in the dark at 27 ± 0.5°C and 70 ± 5% relative humidity for the different experiments reported below.

2.3 | Infection of larvae and collection of hemolymph

Escherichia coli strain K12 (Sigma-Aldrich) and *Micrococcus luteus* ATCC 4698 (Sigma-Aldrich) were used for infecting BSF larvae. Bacteria were grown in 10 mL Luria-Bertani broth overnight at 37°C with shaking at 160 rpm. Subsequently, 1 mL of both cultures was centrifuged at 1620*g* for 15 min and cell pellets were washed with Phosphate Buffered Saline (PBS; 137 mM NaCl, 2.7 mM KCl, 10 mM Na_2HPO_4/KH_2PO_4, pH 7.4). After measuring the optical density at 600 nm of the bacterial suspension (one unit of OD_{600nm} corresponds to about 4×10^8 CFU/mL of *E. coli* and about 2×10^7 CFU/mL of *M. luteus*), cells were suspended and diluted in PBS to the concentration suitable for injection into the larvae (i.e., about 1×10^5 CFU/mL of *E. coli*/*M. luteus* mix) (Bruno et al., 2021).

Last instar larvae were washed with tap water to remove food debris from the cuticle and then with 0.5% sodium hypochlorite (in tap water, v/v) and 70% ethanol (in distilled water, v/v). Insects were injected with 5 µL of the bacterial mix using a Hamilton 700 10-µL syringe (Hamilton). After the injection, larvae were kept under sterile conditions in Petri dishes at 27 ± 0.5°C and 70 ± 5% relative humidity without food.

Hemolymph was collected in plastic tubes on ice by piercing the larvae with a sterile needle between the first and the second metamere. Uninfected larvae (naïve) were used as controls in all the experiments (Bruno et al., 2021). To exclude the potential involvement of HiRNASET2 in wound healing processes, additional controls were conducted by puncturing the larvae with a sterile needle or by injecting them with sterile PBS (Supporting Information).

2.4 | Immunostaining

2.4.1 | Fat body

The fat body was isolated from last instar larvae at 3 and 6 h after the infection, embedded in polyfreeze cryostat embedding medium (Tebubio) added with 20% sucrose (8:2, v/v), frozen in liquid nitrogen, and stored at −80°C until use. Cryosections (7-µm-thick) were obtained with a CM1850 cryostat (Leica) and stored at −20°C until use. After rinsing in PBS, sections were incubated in blocking solution (2% bovine serum albumin [BSA], 0.1% Tween 20 in PBS) for 30 min. Samples were then incubated for 1 h with rabbit anti-RNASET2 diluted 1:150. Finally, samples were incubated for 45 min with a goat anti-rabbit FITC-conjugated antibody (Jackson ImmunoResearch Laboratories; dilution 1:250).

2.4.2 | Hemocytes

15, 30, 60 min and 3 h postinfection, 100 µL of hemolymph were collected, poured onto sterile round coverslips in the dark for 15 min to allow hemocyte adhesion, and then cells were fixed in 4% paraformaldehyde in PBS for 10 min. Samples were first incubated with 2% BSA, 0.1% Tween 20 in PBS for 30 min and then with anti-RNASET2 antibody (dilution 1:300) for 1 h. Finally, samples were incubated with a Cy3-conjugated antirabbit antibody (Abcam; dilution 1:300) for 1 h.

Nuclei were stained with DAPI (100 ng/mL in PBS). Specimens were mounted with Citifluor (Citifluor Ltd) and observed under an Eclipse Ni-U microscope (Nikon) equipped with a DS-SM-L1 digital camera (Nikon). Fluorescent hemocytes were quantified by analyzing 5 different images (50x magnification) randomly selected from each independent experiment. Images were overlayed with Adobe Photoshop. Negative controls were obtained by omitting the primary antibody.

The time points for the isolation and analysis of both fat body and hemocytes used in the present study, as well as for the investigation of the different immunological markers, were selected according to an in-depth, previous characterization of the immune response of BSF larvae (Bruno et al., 2021).

2.5 | SDS-PAGE and western blot

3 and 6 h after the infection, the fat body was isolated and homogenized with T10 basic ULTRA-TURRAX (IKA) in RIPA buffer (150 mM NaCl, 2% NP 40, 0.5% sodium deoxycholate, 0.1% SDS, and 50 mM Tris-HCl, pH 8.0) (1 mL/0.14 g of tissue), in which protease and phosphatase inhibitors (Cell Signaling Technology) were added. The homogenate was centrifuged at 15,000*g* for 15 min at 4°C and the supernatant was collected.

Hemocytes and cell-free fraction were obtained by centrifuging the hemolymph collected at 15, 30, 60 min and 3 h after the infection (450*g* for 5 min at 4°C). Proteins in the cell-free fraction (i.e., the supernatant obtained after centrifugation) (CFF) were precipitated using a methanol-chloroform solution (4:1 v/v) (Rose et al., 2023) and resuspended in 4X loading buffer (0.1 M Tris-HCl, 40% glycerol, 20% SDS,

β-mercaptoethanol). Protein concentration in the fat body and hemocyte samples was determined through Bradford assay (Bradford, 1976). After boiling, protein samples were loaded on a 12% Tris-glycine acrylamide gel (40 µg protein/lane for fat body and hemocytes, 20 µL sample/lane for CFF). Proteins were then transferred to a 0.45-µm nitrocellulose membrane (GE Healthcare Life Sciences), incubated for 2 h in 5% milk in Tris Buffered Saline (TBS, 50 mM Tris-HCl, 150 mM NaCl, pH 7.5), and then for 1 h with anti-RNASET2 or with anti-GAPDH (Proteintech) antibodies (dilution 1:3000 for RNASET2 and 1:2500 for GAPDH) (Baranzini et al., 2019; Bruno et al., 2019). After washes with TBS, membranes were probed for 1 h with an anti-rabbit HRP-conjugated antibody (Jackson ImmunoResearch Laboratories) (dilution 1:5000 for RNASET2 and 1:7500 for GAPDH). Immunocomplexes were revealed with Luminol LiteAblot® PLUS Enhanced Chemiluminescent Substrate (EuroClone). Densitometric analysis was performed with ImageJ. Briefly, after subtracting background, the total pixel counts for HiRNASET2 were divided by the respective total pixel counts of HiGAPDH bands for normalization. Results were expressed as arbitrary densitometry units (ADU). Experiments were performed in triplicate.

2.6 | Immunogold labeling

30 min after the infection, hemolymph was isolated and fixed in 2% glutaraldehyde in 0.1 M Na-cacodylate buffer (pH 7.4) overnight at 4°C. After centrifugation at 200*g* for 10 min, hemocytes were postfixed with 2% osmium tetroxide in 0.1 M Na-cacodylate buffer for 20 min. Sample was dehydrated in an ascending ethanol series and embedded in Epon-Araldite 812 mixture resin (Sigma-Aldrich). Sections (70-nm-thick) were obtained using a Leica Reichert Ultracut S (Leica) and collected on gold grids (300 mesh). After etching with 3% NaOH in ethanol, they were incubated with 1% BSA, 0.1% Tween 20 in PBS for 30 min, and then with rabbit anti-RNASET2 antibody (diluted 1:50) for 1 h. After two washes with PBS, samples were incubated with 10 nm gold-conjugated goat antirabbit antibody (GE Healthcare Life Sciences; dilution 1:50) for 1 h. They were postfixed with 0.5% glutaraldehyde in PBS for 5 min, counterstained with uranyl acetate, and observed under a JEM-1010 transmission electron microscope (Jeol) equipped with a Morada digital camera (Olympus) (Centro di Ricerca e Trasferimento Tecnologico [CRIETT], University of Insubria). Controls were obtained by omitting the primary antibody. Experiments were performed in triplicate.

2.7 | qRT-PCR

3 and 6 h after the infection, BSF larvae were anesthetized on ice, dissected, and the fat body was isolated, frozen in liquid nitrogen, and stored at −80°C until use. Hemolymph was isolated from larvae at 15, 30, 60 min and 3 h postinfection and placed in sterile Petri dishes filled with sterile Schneider's insect medium for 20 min to allow cell adhesion. Hemocytes were washed twice with Schneider's insect medium to remove fat body debris, then scraped with TRIzol reagent (Life Technologies), and stored at −80°C until use. RNA was extracted from 30 to 40 mg of fat body and 1×10^6 hemocytes/mL with 1 mL of TRIzol reagent, as reported in Bruno et al. (2021). The RNA quantity was determined by using NanoDrop (Thermo Fisher Scientific) and RNA quality was verified through gel electrophoresis. Two micrograms of RNA was retrotranscribed using M-MLV reverse transcriptase (Life Technologies). Primers used for qRT-PCR (Table 1) were designed on sequences of *HiRNASET2* and ribosomal protein L5 (*HiRPL5*) derived from a *de novo H. illucens* midgut transcriptome (Bonelli et al., 2020) (accession number: ERP122672).

Real-Time PCR was performed using the iTaq Universal SYBR Green Supermix (Bio-Rad) in a CFX Connect Real-Time PCR Detection System (Bio-Rad). Expression levels were determined using the $2^{-\Delta\Delta Ct}$ method. Each value was the result of five replicates.

TABLE 1 Sequence of primers used in this study.

Gene name	Accession number	Contig number	Primer sequence
HiRNASET2	XM038071081.1	TRINITY_DN9106_C0_G1_I2	F: CAACGAAATACGGGACGGTG R: AAATCGGCTTCTACGCTTGG
HiRPL5	ERP122672	TRINITY_DN8551_C0_G1_I2	F: AGTCAGTCTTTCCCTCACGA R: GCGTCAACTCGGATGCTA

2.8 | Synthesis of the putative HiRNASET2 antimicrobial peptide and evaluation of its activity

The putative antimicrobial peptide (KVITNCHISKPVQ), identified via bioinformatic analysis in the HiRNASET2 sequence, was synthetized by the Proteomics and Peptide Synthesis Facility (University of Padova). The lyophilized peptide was resuspended in 1 mL of autoclaved MilliQ water (final molarity: 3.4 mM).

To test the antibacterial activity of the peptide, *E. coli* and *M. luteus* were grown as described above ("Infection of larvae and collection of hemolymph"). As previously tested for HvRNASET2 (Baranzini et al., 2020b) and other transferase-type RNases (Torrent et al., 2009; Yu et al., 2015) peptides, 6 µL of 3.4 or 0.34 mM of peptide solution were added to 200 µL of each bacteria suspension (final concentration of 10 and 100 µM, respectively). MilliQ water was used as control. Bacteria were then incubated overnight at room temperature with mild agitation to allow the interaction of the synthetic peptide with the cells. The possible antimicrobial effect of the peptide was evaluated by viable count technique (Baranzini et al., 2020b).

2.9 | Statistical analysis

Statistical analysis was conducted with GraphPad Prism version 7.00. One-way ANOVA followed by Tukey's multiple-comparison post hoc test was used to check statistical differences between groups, which were considered significant at $p < 0.05$. The normality of the data was checked by using the Shapiro–Wilk test.

3 | RESULTS

3.1 | In silico characterization of HiRNASET2

Bioinformatic analyses conducted on the amino acid sequence (Figure 1a) revealed that HiRNASET2 consisted of 287 amino acids, with a molecular weight of 32.87 kDa. Two specific, and highly conserved, Rh/T2/S ribonucleases active sites (CAS I and CAS II) were identified using the ScanProsite database tool. These domains were located in position Trp75-Thr83 (WTIHGIWPT) and Lys127-Ala139 (LWEHEWLKHGTCA) and contained two catalytically functional histidine residues (His78 and His135). This evidence, described also for other T2 RNases (Baranzini et al., 2020b), was confirmed by ConSurf analyses (Figure 1a) and by Clustal Omega multiple alignments with T2 sequences of other invertebrates (Supporting Information S1: Figure 1A,B). The three-dimensional structure obtained with the I-TASSER modeling predictive software confirmed the typical T2 RNases spatial organization, which consisted of a α+β secondary structure core motif composed of five central β-sheet surrounded by six helical regions (Figure 1b). The two CAS domains were located in the central β2-strand and in the α3-helix (Figure 1b). The quality of the 3D model was then

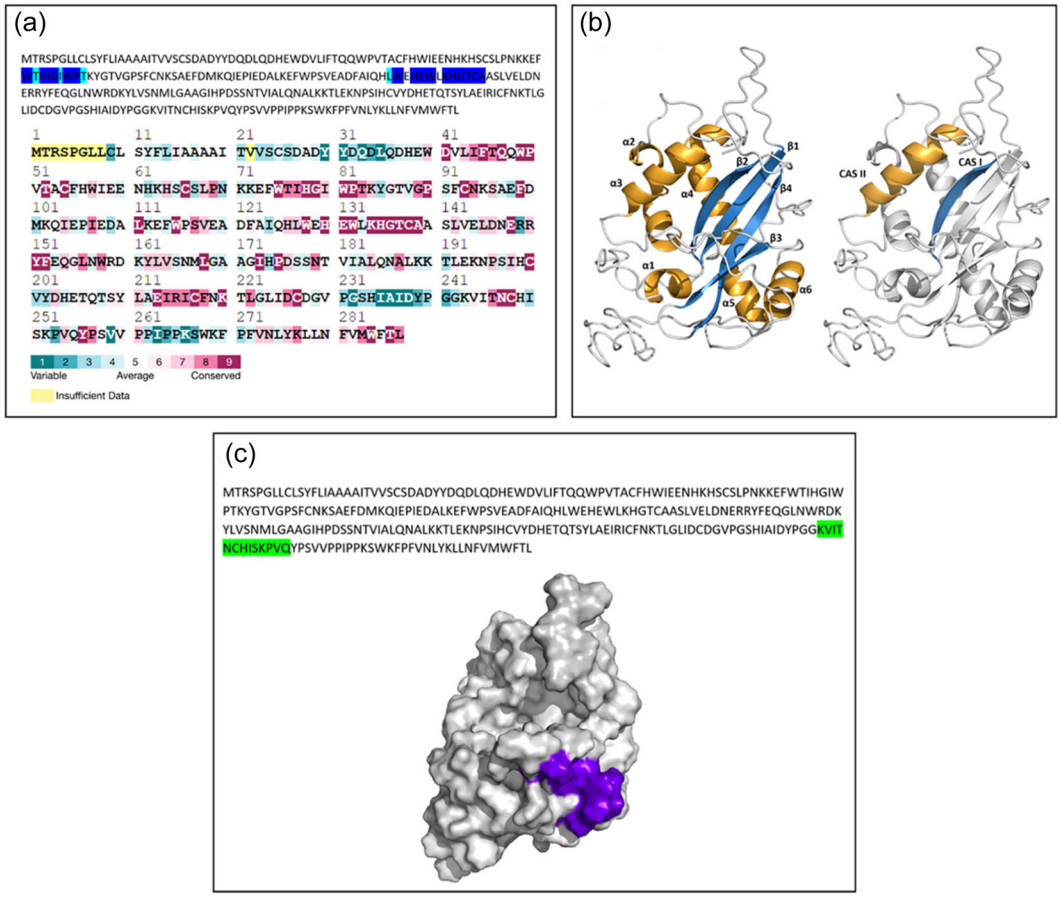

FIGURE 1 In silico analysis of HiRNASET2. (a) The primary HiRNASET2 amino acid sequence was obtained by NCBI (accession number: XM038071081.1). Conserved CAS I and CAS II domains are highlighted in blue. The level of conservation of every single amino acid was identified by ConSurf analysis. (b) HiRNASET2 α-helices and β-strands are represented in yellow and blue, respectively. The conserved CAS I and CAS II domains are located in the central β2-strand and in the parallel α3-helix, respectively. (c) HiRNASET2 antimicrobial peptide in the C-terminal region is indicated in green. Its localization on the external surface can be observed in the 3D structure.

analyzed through graphical alignment with the human RNASET2 (PDB code: 3T0O) (Supporting Information S1: Figure 2A) and the quality of the 3D model was evaluated through the QMEANDisCo mean value (Supporting Information S1: Figure 2B).

The prediction of potential HiRNASET2 functional sequences and the putative enzyme cellular localization were performed through specific bioinformatic tools. SignalP-6.0 revealed the presence of a signal peptide in the N-terminal region, composed of 25 amino acids (MTRSPGLLCLSYFLIAAAAITVVSC) (Supporting Information S1: Figure 2C). Moreover, DeepLoc 2.0, used to predict possible cellular location of eukaryotic proteins, suggested lysosome as HiRNASET2 localization (Supporting Information S1: Figure 2D). Finally, since some T2 RNase homologs have been demonstrated to be directly involved in counteracting bacteria, our analyses focused on the identification of putative antimicrobial peptides in the HiRNASET2 sequence. The AMPA algorithm revealed a sequence of 13 amino acids (KVITNCHISKPVQ) in the C-terminal terminal protein region (position: Lys243-Gln255) that presented an encouraging probability score (Figure 1c). 3D analyses confirmed that this peptide was localized on the external surface of the enzyme (Figure 1c).

3.2 | HiRNASET2 expression and localization, and antimicrobial activity of putative HiRNASET2 peptide

To evaluate the possible involvement of HiRNASET2 in the response of *H. illucens* against pathogens, its expression and localization were assessed in the fat body and hemocytes, the two main body districts involved in the insect immune response, in larvae challenged with bacterial infection.

qRT-PCR analysis revealed that *HiRNASET2* was constitutively expressed in the fat body, and no significant variations in mRNA levels were observed at 3 and 6 h after the infection (Figure 2a) ($p = 0.4874$). Similarly, both western blot (Figure 2b,b') ($p = 0.0840$) and immunostaining (Figure 2c–f) revealed no induction of T2 ribonuclease synthesis in infected larvae, confirming that the production of HiRNASET2 in this tissue was not related to the presence of bacteria in the hemolymph. Differently, a prompt increase in mRNA levels was observed in hemocytes 15 min after the infection, followed by a reduction to basal levels at 30 and 60 min and a subsequent, significant increase 180 min after the injection of bacteria (Figure 3a) ($p < 0.0001$). A completely different trend was observed in the hemocytes of larvae punctured with a sterile needle or injected with sterile PBS (Supporting Information S1: Figure 3), in which an increase in *HiRNASET2* expression levels was never detected. In addition, the evaluation of HiRNASET2 protein, both in the hemocytes and secreted in the hemolymph (i.e., CFF), revealed a peak 30 min after the infection both in the hemocytes and CFF (Figure 3b,b',c,c') ($p < 0.0001$).

Immunostaining performed on hemocytes at different time points after the infection confirmed western blot results. In fact, a time-dependent increase in HiRNASET2 levels was observed up to 30 min after the infection (Figure 3d–f). The signal then progressively decreased (Figure 3g–i), as demonstrated by quantitative analysis (Figure 3j) ($p < 0.05$). The positive signal was detected in the majority of cells, indicating that hemocytes responsible for HiRNASET2 synthesis were probably plasmatocytes, comprising approximately 90% of circulating cells in *H. illucens* (Bruno et al., 2023).

The spot localization pattern observed in immunostainings, as well as the high levels of secreted HiRNASET2 in the CFF hemolymph, suggested the presence of this ribonuclease in cytoplasmic vesicles and in the extracellular environment, respectively. Its ultrastructural localization was confirmed through immunogold labeling. TEM analysis revealed that, 30 min after the infection, HiRNASET2 was localized both in the lysosomes of plasmatocytes (Figure 4a,b) and on the outer surface of bacteria circulating in the hemolymph (Figure 4c).

Finally, to evaluate the possible involvement of HiRNASET2 in the immune response of the larvae to bacterial infection, the effect of the putative HiRNASET2 antimicrobial peptide, predicted via bioinformatic analyses (Figure 1), was assessed in vitro on *E. coli* and *M. luteus*. The incubation of bacteria with the synthetic peptide influenced the growth of both strains. In particular, after 24 h of incubation, a reduction in the number of colonies of both microorganisms compared to controls was recorded (Figure 5) (*E. coli*: $p = 0.0057$; *M. luteus*: $p = 0.0059$).

4 | DISCUSSION

Insects have emerged as a promising source of antimicrobial molecules with diverse applications. Their unique ecological niches and evolutionary adaptations have endowed them with a plethora of defensive mechanisms against microbial threats, including bacteria, fungi, and viruses. These molecules, ranging from peptides to small organic compounds, exhibit potent antimicrobial properties and demonstrate efficacy against drug-resistant pathogens (Eleftherianos et al., 2021; Tettamanti & Bruno, 2024). Harnessing these natural defenses presents an exciting avenue for developing novel antimicrobial agents, offering alternatives to conventional antibiotics plagued by resistance issues. BSF is no exception since dozens of AMPs, exhibiting remarkable potency and specificity, and a broad spectrum of action against bacteria and fungi, have been identified in this insect (Bruno et al., 2021; Moretta et al., 2020; Scieuzo et al., 2023; Vogel et al., 2018). However, although several studies demonstrated the antimicrobial activity of BSF hemolymph (Candian et al., 2023; Scieuzo et al., 2023; Vogel et al., 2018), encompassing

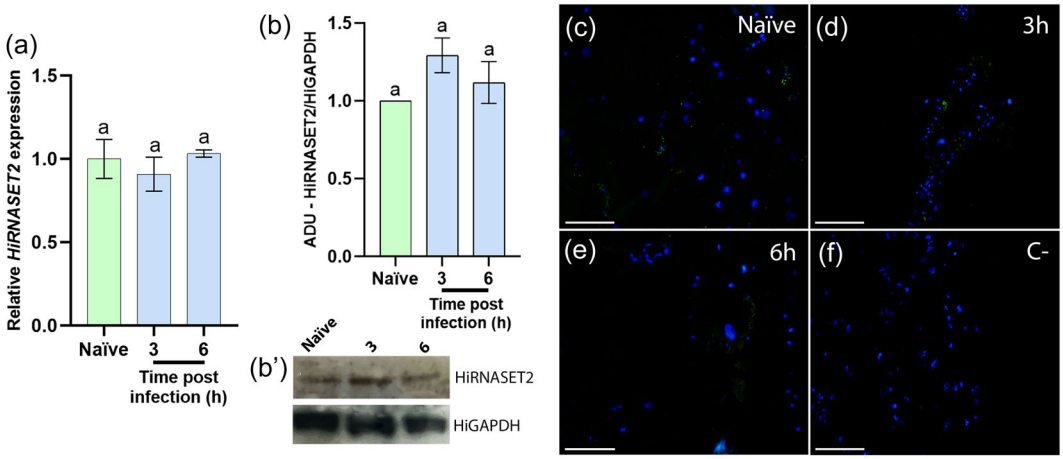

FIGURE 2 HiRNASET2 expression and localization in *Hermetia illucens* fat body at different time points after bacterial infection. (a,b,b') qRT-PCR and western blot analyses of the fat body of naïve and infected larvae. (c–f) HiRNASET2 immunolocalization in naïve larvae (c), and larvae 3 (d) and 6 (e) h after bacterial infection. (f) Negative control. Bars: 50 μm (c–f). Values represent mean ± s.e.m. Different letters indicate statistically significant differences among treatments (one-way ANOVA: (a) $F_{2-32} = 0.7351$, $p = 0.4874$; (b) $F_{2-6} = 3.850$, $p = 0.0840$).

diverse aspects of the cellular and humoral response (Bruno et al., 2021, 2023; von Bredow et al., 2022; Zdybicka-Barabas et al., 2017), information on molecules and regulators underpinning the strong antibacterial response of BSF larvae is still scarce. Based on these premises, the present study focused the attention on enzymes belonging to the T2 RNase family due to their ability to modulate the host defence, especially during bacterial infections, presenting also antimicrobial domains able to affect microorganisms' viability. In particular, we assessed the ability of HiRNASET2 to counteract Gram-negative and Gram-positive bacteria by means of in silico and in vitro analyses.

A first bioinformatic characterization of the primary amino acid sequence and 3D secondary structure revealed many similarities between *H. illucens* T2 ribonuclease and other members of the T2 RNases family. The presence of the two conserved Rh/T2/S ribonuclease-specific active sites, namely CAS I and CAS II, was confirmed by the ScanProsite server. The two domains CAS I and CAS II, located in positions Trp75-Thr83 and Lys127-Ala139, are typically involved in the enzymatic housekeeping role of T2 enzymes, that is the control of RNA processing or degradation (Greulich et al., 2019). The predicted three-dimensional conformation confirms a typical α+β structural organization, with a central core of β-sheets surrounded by several α-helices. The functional relevance of these potential catalytic sites was confirmed by the presence of two histidine residues (His78 and His135), which are involved in the catalytic activity in both CAS sites (Irie, 1997; Kawata et al., 1990). This evidence was validated by the high similarity retrieved through multiple sequence alignments with several invertebrate T2 members. Of note, AMPA software predicted the presence of an amino acid motif with potential antibacterial properties in the C-terminal region, with a value of isoelectric point (9.9) and total positive net charge (+2.00) typical of AMPs (Torrent et al., 2011). These properties could confer to this motif a binding capability to negatively charged bacterial membranes through electrostatic interactions (Yeaman & Yount, 2003), which can trigger the damage of the bacterial membrane and the activation of intracellular processes leading to the death of the microorganism (Geitani et al., 2020). To verify this hypothesis, we tested the antimicrobial activity of the predicted peptide only upon use of stressful conditions for bacteria, that is, administration of high peptide concentrations to nongrowing cells (bacteria maintained overnight in starvation and nonoptimal growing temperature). This experimental set-up showed a moderate antibacterial effect of the isolated peptide. Although further investigations are necessary to address the underlying action mechanism/s among the most recognized

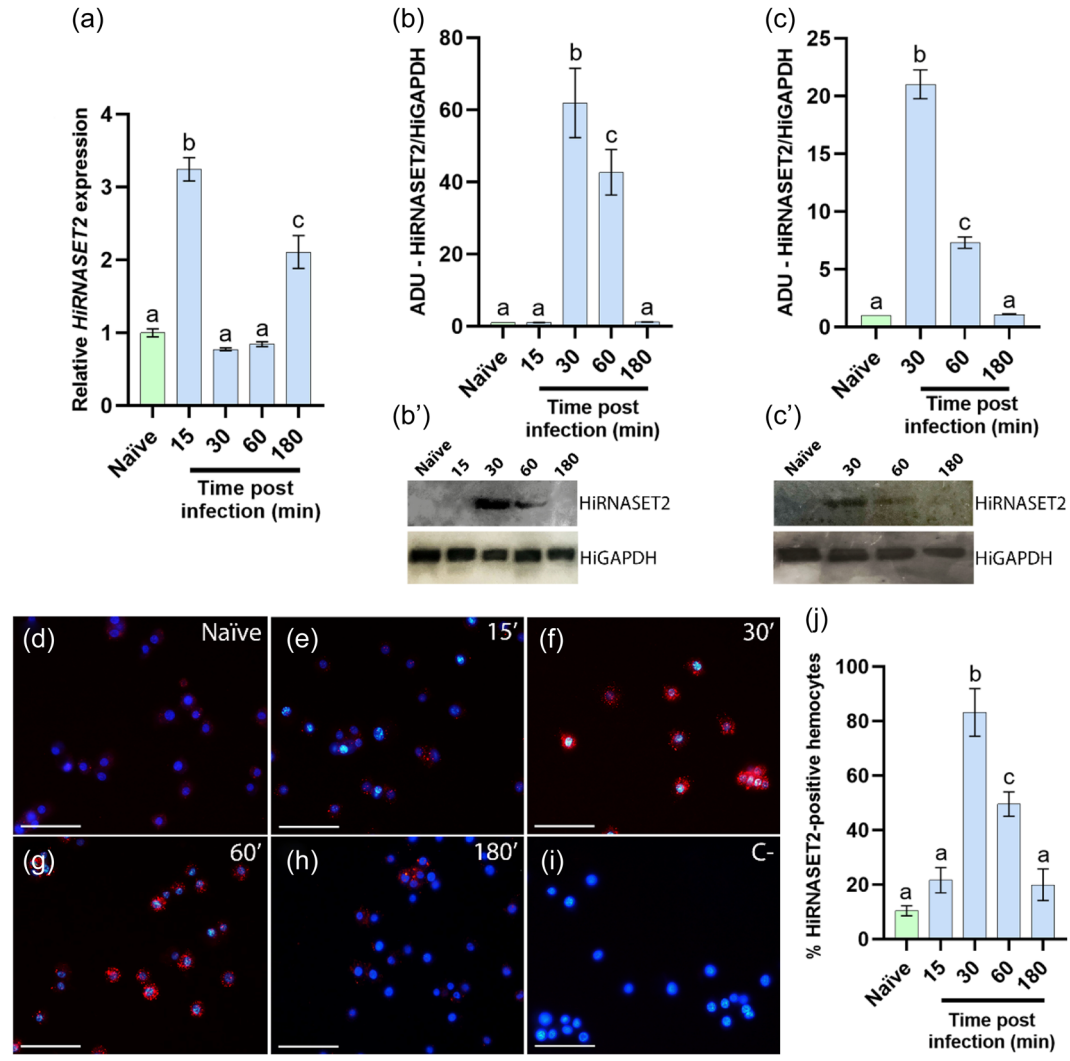

FIGURE 3 HiRNASET2 expression and localization in *Hermetia illucens* hemocytes and hemolymph at different time points after bacterial infection. (a,b,b') qRT-PCR and western blot analyses of larval hemocytes. (c and c') Western blot analysis of the CFF. (d–i) HiRNASET2 localization (red signal) in hemocytes from naïve larvae (d) and larvae at 15, 30, 60, and 180 min post infection (e–h). (i) Negative control. (j) Percentage of HiRNASET2-positive hemocytes. Bars: 50 μm (d–i). Values represent mean ± s.e.m. Different letters indicate statistically significant differences among treatments (one-way ANOVA: (a) $F_{4-10} = 213.5$, $p < 0.0001$; (b) $F_{4-10} = 39.68$, $p < 0.0001$; (c) $F_{3-8} = 590$, $p < 0.0001$; (j) $F_{4-10} = 85.58$, $p < 0.05$).

ones (Zhou et al., 2024), the results observed both in Gram-negative and Gram-positive models, suggest the hypothesis of the involvement of bilayer disruption rather than the interference with nucleic acid, protein, and cell wall synthesis. In addition, the presence of gold particles on the bacterial surface revealed by immunogold supports the hypothesis of a direct interaction between HiRNASET2 and cell wall components. Such interaction could be mediated by the C-terminal peptide, which might confer an antimicrobial role to this enzyme, as observed for other ribonucleases such as leech HvRNASET2 (Baranzini et al., 2020b) and human RNase 3 (ECP) (Torrent et al., 2009), classified as antimicrobial proteins and playing a key role in the first line of host defense against invading pathogens.

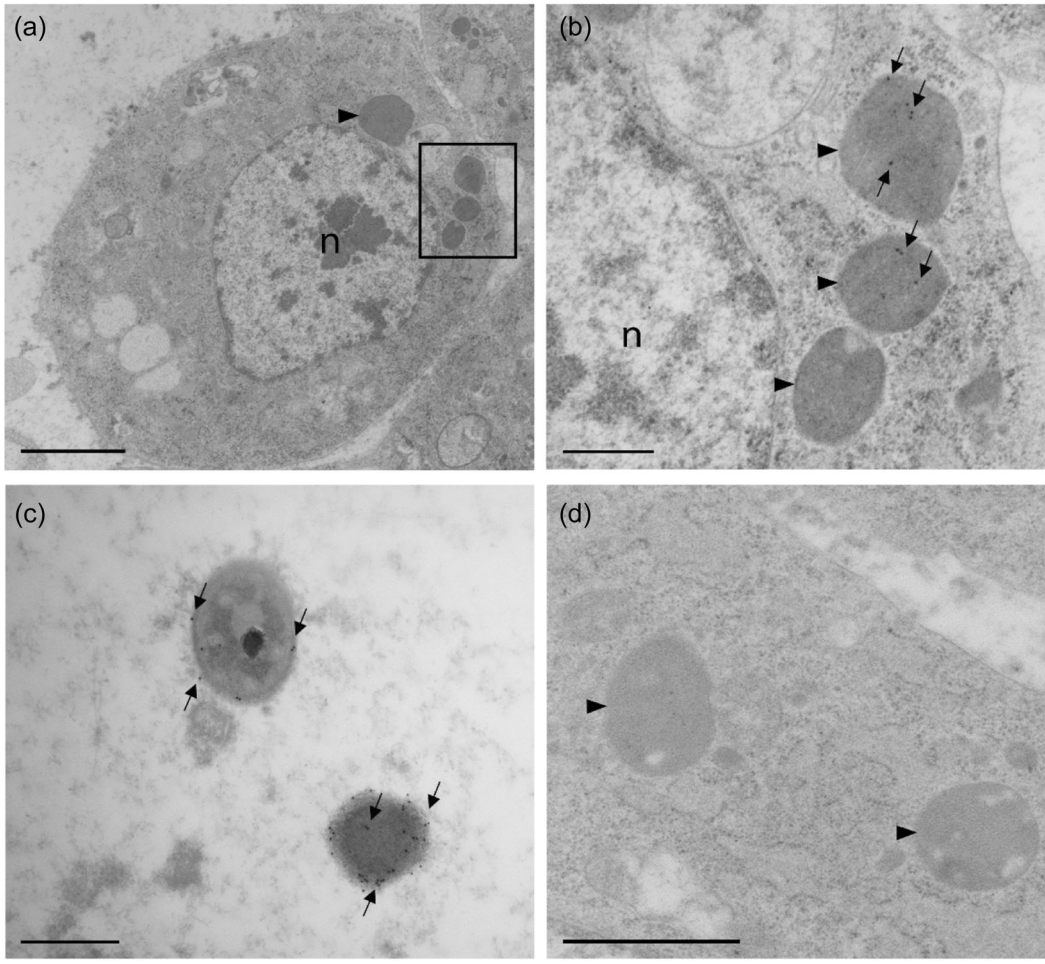

FIGURE 4 Ultrastructural localization of HiRNASET2 in *Hermetia illucens* hemocytes. (a and b) HiRNASET2 localization in lysosomes of plasmatocytes and (c) on the surface of bacteria in the hemolymph. (d) Negative control. Arrowheads: lysosomes; arrows: gold particles; n: nucleus. (b) is a magnification of the area delineated in (a). Bars: 2 μm (a), 1 μm (d), 0.5 μm (b and c).

During inflammatory processes, T2 enzymes are specifically secreted by immune cells (Acquati et al., 2019; Baranzini et al., 2019). Similarly, HiRNASET2 is constitutively produced by hemocytes in naïve larvae, and its production increases after 30 min from the injection of the *E. coli*/*M. luteus* bacterial mix. A prompt increase in *HiRNASET2* mRNA levels already 15 min after the infection indicates an early activation of this enzyme. A second boost of mRNA expression at later stages (3 h post infection) might support the synthesis of this T2 ribonuclease to counteract remaining pathogens still alive in the larva or to better cope with a potential, second infection, as already observed for BSF AMPs (Bruno et al., 2021). Unlike in leeches (Baranzini et al., 2021; Baranzini et al., 2020c), RNASET2 does not appear to have any role in wound healing in *H. illucens*, as suggested by the lack of increase in its RNA levels following needle puncture. This is probably related to the different cellular and molecular mechanisms that are implemented by the two animal models during tissue regeneration. In particular, wound regeneration in insects does not involve the production and remodeling of a collagen scaffold, but the initial formation of a plug made up of fat body fragments, hemocytes, and melanin, that is followed by the migration of epidermal cells toward the wound to form a new cuticle, thus restoring tegument integrity (Krautz et al., 2014). Interestingly, HiRNASET2 appears to play a different role in the fat body, despite

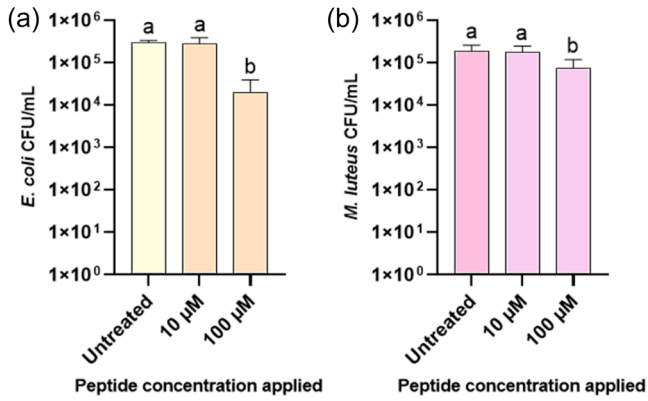

FIGURE 5 Antimicrobial activity of the putative HiRNASET2 antimicrobial peptide. (a) Cellular viability of *Escherichia coli* and (b) *Micrococcus luteus* after 24 h of peptide incubation. Untreated cells were used as controls (Untreated). Values represent the mean ± s.e.m. Different letters indicate statistically significant differences among treatments (one-way ANOVA: (a) $F_{2-6} = 13.79$, $p = 0.0057$; (b) $F_{2-6} = 6.096$, $p = 0.0059$).

the active role of this tissue in the immune response of the larva (Bruno et al., 2021). Indeed, this enzyme is basally expressed in this tissue, but its protein levels do not increase following bacterial infection. Probably, as reported for *D. melanogaster* RNase X25, HiRNASET2 maintains cellular homeostasis in the fat body by recycling rRNA (Ambrosio et al., 2014; MacIntosh, 2011).

Immunostaining performed on hemocytes revealed HiRNASET2 localization in vesicles, in particular lysosomes, as previously suggested (Campomenosi et al., 2006; Haud et al., 2011) and by the acidic pH needed for T2 RNases optimal activity. This hypothesis is corroborated by bioinformatic prediction and immunogold, which confirm the presence of this ribonuclease in electron-dense granules similar to lysosomes and phagolysosomes (Bruno et al., 2023). Furthermore, the localization of HiRNASET2 on the surface of bacteria circulating in the hemolymph leads to the hypothesis that this enzyme in BSF larvae could act as: (i) a clean-up molecule of exogenous RNA inside lysosomes and (ii) an alarm molecule or an opsonin, transmitting a danger signal, such as the presence of bacteria into the hemocoel, to promote the activation of phagocytosis by hemocytes (Baranzini et al., 2019). This second mechanism is similar to that of other C-type lectins detected in other arthropods such as shrimps of the genus *Penaeus* and in the insect *Manduca sexta*, where they not only agglutinate *E. coli* cells but also bind to LPS to opsonize microbes, promoting phagocytosis and inducing the activation of phenoloxidase system (Luo et al., 2006; Yu & Kanost, 2000).

5 | CONCLUSION

This study provides new information on the BSF immune system and expands knowledge of the defense mechanisms of Diptera. Additionally, it provides a starting platform for future studies on T2 enzymes and their involvement in immune responses, not only in insects but also in other invertebrates. A further characterization of the potential antimicrobial peptide of HiRNASET2 is not only scientifically intriguing, but also holds potential perspective as it could confer added value to BSF-based feedstuff to enhance animal resistance to pathogens.

AUTHOR CONTRIBUTIONS

Sara Caramella: Data curation; formal analysis; investigation; writing—original draft preparation. **Nicolò Baranzini**: Conceptualization; data curation; formal analysis; investigation; methodology; software; supervision; visualization;

writing—original draft preparation; writing—review & editing. **Daniele Bruno**: Conceptualization; data curation; validation; supervision; visualization; writing—review & editing. **Viviana Teresa Orlandi**: Data curation; formal analysis; investigation; writing—original draft preparation; writing—review & editing. **Amr Mohamed**: Writing—review & editing. **Fabrizion Bolognese**: Investigation. **Annalisa Grimaldi**: Conceptualization; supervision; writing—original draft preparation; writing—review & editing. **Gianluca Tettamanti**: Conceptualization; funding acquisition; project administration; supervision; writing—review & editing.

ACKNOWLEDGMENTS

This work was supported by PRIN 2022 PNRR (Prot. P2022MZAF8; "Finanziamento dell'Unione Europea—NextGenerationEU—PNRR Missione 4, Componente 2, Investimento 1.1"). We are grateful to Prof. Francesco Acquati (University of Insubria, Italy) for providing anti-RNASET2 antibody. Sara Caramella is a PhD student of the "Life Science and Biotechnology" course at University of Insubria. Amr Mohamed is a research fellow—not a formal employee—at the King Saud University Museum of Arthropods (KSMA), King Saud University. Open access publishing facilitated by Universita degli Studi dell'Insubria, as part of the Wiley - CRUI-CARE agreement.

CONFLICT OF INTEREST STATEMENT

The authors declare no conflict of interest.

ORCID

Sara Caramella https://orcid.org/0009-0001-1843-5438
Nicolò Baranzini https://orcid.org/0000-0001-6996-4797
Daniele Bruno https://orcid.org/0000-0002-2550-3267
Viviana Teresa Orlandi https://orcid.org/0000-0001-6010-2840
Amr Mohamed https://orcid.org/0000-0003-2788-5534
Annalisa Grimaldi https://orcid.org/0000-0002-9258-7595
Gianluca Tettamanti https://orcid.org/0000-0002-0665-828X

REFERENCES

Acquati, F., Monti, L., Lualdi, M., Fabbri, M., Sacco, M.G., Gribaldo, L. et al. (2011) Molecular signature induced by RNASET2, a tumor antagonizing gene, in ovarian cancer cells. *Oncotarget*, 2, 477–484.

Acquati, F., Mortara, L., De Vito, A., Baci, D., Albini, A., Cippitelli, M. et al. (2019) Innate immune response regulation by the human RNASET2 tumor suppressor gene. *Frontiers in Immunology*, 10, 488255.

Ambrosio, L., Morriss, S., Riaz, A., Bailey, R., Ding, J. & MacIntosh, G.C. (2014) Phylogenetic analyses and characterization of RNase X25 from *Drosophila melanogaster* suggest a conserved housekeeping role and additional functions for RNase T2 enzymes in protostomes. *PLoS One*, 9, e105444.

Baranzini, N., Monti, L., Vanotti, M., Orlandi, V.T., Bolognese, F., Scaldaferri, D. et al. (2019) AIF-1 and RNASET2 play complementary roles in the innate immune response of medicinal leech. *Journal of Innate Immunity*, 11, 150–167.

Baranzini, N., Pulze, L., Reguzzoni, M., Roncoroni, R., Orlandi, V.T., Tettamanti, G. et al. (2020b) 3D reconstruction of *Hv*RNASET2 molecule to understand its antibacterial role. *International Journal of Molecular Sciences*, 21, 9722.

Baranzini, N., Pulze, L., Tettamanti, G., Acquati, F. & Grimaldi, A. (2021) *Hv*RNASET2 regulate connective tissue and collagen I remodeling during wound healing process. *Frontiers in Physiology*, 12, 632506.

Baranzini, N., De Vito, A., Orlandi, V.T., Reguzzoni, M., Monti, L., De Eguileor, M. et al. (2020a) Antimicrobial role of RNASET2 protein during innate immune response in the medicinal leech *Hirudo verbana*. *Frontiers in Immunology*, 11, 486907.

Baranzini, N., Weiss-Gayet, M., Chazaud, B., Monti, L., de Eguileor, M., Tettamanti, G. et al. (2020c) Recombinant HvRNASET2 protein induces marked connective tissue remodelling in the invertebrate model *Hirudo verbana*. *Cell and Tissue Research*, 380, 565–579.

Berezin, C., Glaser, F., Rosenberg, J., Paz, I., Pupko, T., Fariselli, P. et al. (2004) ConSeq: the identification of functionally and structurally important residues in protein sequences. *Bioinformatics*, 20, 1322–1324.

Berman, H.M., Battistuz, T., Bhat, T.N., Bluhm, W.F., Bourne, P.E., Burkhardt, K. et al. (2002) The protein data bank. *Acta Crystallographica. Section D, Biological Crystallography*, 58, 899–907.

Bonelli, M., Bruno, D., Brilli, M., Gianfranceschi, N., Tian, L., Tettamanti, G. et al. (2020) Black soldier fly larvae adapt to different food substrates through morphological and functional responses of the midgut. *International Journal of Molecular Sciences*, 21, 4955.

Bradford, M.M. (1976) A rapid and sensitive method for the quantitation of microgram quantities of protein utilizing the principle of protein-dye binding. *Analytical Biochemistry*, 72, 248–254.

von Bredow, Y.M., Müller, A., Popp, P.F., Iliasov, D. & von Bredow, C.R. (2022) Characterization and mode of action analysis of black soldier fly (*Hermetia illucens*) larva-derived hemocytes. *Insect Science*, 29, 1071–1095.

Bruno, D., Bonelli, M., Cadamuro, A.G., Reguzzoni, M., Grimaldi, A., Casartelli, M. et al. (2019) The digestive system of the adult *Hermetia illucens* (Diptera: Stratiomyidae): morphological features and functional properties. *Cell and Tissue Research*, 378, 221–238.

Bruno, D., Montali, A., Gariboldi, M., Wrońska, A.K., Kaczmarek, A., Mohamed, A. et al. (2023) Morphofunctional characterization of hemocytes in black soldier fly larvae. *Insect Science*, 30, 912–932.

Bruno, D., Montali, A., Mastore, M., Brivio, M.F., Mohamed, A., Tian, L. et al. (2021) Insights into the immune response of the black soldier fly larvae to bacteria. *Frontiers in Immunology*, 12, 745160.

Campomenosi, P., Salis, S., Lindqvist, C., Mariani, D., Nordström, T., Acquati, F. et al. (2006) Characterization of RNASET2, the first human member of the Rh/T2/S family of glycoproteins. *Archives of Biochemistry and Biophysics*, 449, 17–26.

Candian, V., Savio, C., Meneguz, M., Gasco, L. & Tedeschi, R. (2023) Effect of the rearing diet on gene expression of antimicrobial peptides in *Hermetia illucens* (Diptera: Stratiomyidae). *Insect Science*, 30, 933–946.

Castellanos, N., Martínez, L.C., Silva, E.H., Teodoro, A.V., Serrão, J.E. & Oliveira, E.E. (2017) Ultrastructural analysis of salivary glands in a phytophagous stink bug revealed the presence of unexpected muscles. *PLoS One*, 12, e0179478.

Ceccotti, C., Bruno, D., Tettamanti, G., Branduardi, P., Bertacchi, S., Labra, M. et al. (2022) New value from food and industrial wastes—bioaccumulation of omega-3 fatty acids from an oleaginous microbial biomass paired with a brewery by-product using black soldier fly (*Hermetia illucens*) larvae. *Waste Management*, 143, 95–104.

De, A. & Funatsu, G. (1992) Crystallization and preliminary X-ray diffraction analysis of a plant ribonuclease from the seeds of the bitter gourd *Momordica charantia*. *Journal of Molecular Biology*, 228, 1271–1273.

Deshpande, R.A. & Shankar, V. (2002) Ribonucleases from T2 family. *Critical Reviews in Microbiology*, 28, 79–122.

Eleftherianos, I., Zhang, W., Heryanto, C., Mohamed, A., Contreras, G., Tettamanti, G. et al. (2021) Diversity of insect antimicrobial peptides and proteins—a functional perspective: a review. *International Journal of Biological Macromolecules*, 191, 277–287.

Geitani, R., Moubareck, C.A., Xu, Z., Karam Sarkis, D. & Touqui, L. (2020) Expression and roles of antimicrobial peptides in innate defense of airway mucosa: potential implication in cystic fibrosis. *Frontiers in Immunology*, 11, 527679.

Greulich, W., Wagner, M., Gaidt, M.M., Stafford, C., Cheng, Y., Linder, A. et al. (2019) TLR8 is a sensor of RNase T2 degradation products. *Cell*, 179, 1264–1275.

Haud, N., Kara, F., Diekmann, S., Henneke, M., Willer, J.R., Hillwig, M.S. et al. (2011) RNASET2 mutant zebrafish model familial cystic leukoencephalopathy and reveal a role for RNase T2 in degrading ribosomal RNA. *Proceedings of the National Academy of Sciences*, 108, 1099–1103.

Hogsette, J.A. (1992) New diets for production of house flies and stable flies. *Journal of Economic Entomology*, 85, 2291–2294.

Horiuchi, H., Yanai, K., Takagi, M., Yano, K., Wakabayashi, E., Sanda, A. et al. (1988) Primary structure of a base non-specific ribonuclease from *Rhizopus niveus*. *The Journal of Biochemistry*, 103, 408–418.

Inokuchi, N., Koyama, T., Sawada, F. & Irie, M. (1993) Purification, some properties, and primary structure of base non-specific ribonucleases from *Physarum polycephalum*. *The Journal of Biochemistry*, 113, 425–432.

Irie, M. (1997) RNase T1/RNase T2 family RNases. *Ribonucleases*, 101–130.

Irie, M. (1999) Structure-function relationships of acid ribonucleases: lysosomal, vacuolar, and periplasmic enzymes. *Pharmacology & Therapeutics*, 81, 77–89.

Kawata, Y., Sakiyama, F., Hayashi, F. & Kyogoku, Y. (1990) Identification of two essential histidine residues of ribonuclease T2 from *Aspergillus oryzae*. *European Journal of Biochemistry*, 187, 255–262.

Kawata, Y., Sakiyama, F. & Tamaoki, H. (1988) Amino-acid sequence of ribonuclease T2 from *Aspergillus oryzae*. *European Journal of Biochemistry*, 176, 683–697.

Kobayashi, H., Inokuchi, N., Koyama, T., Watanabe, H., Iwama, M., Ohgi, K. et al. (1992) Primary structure of a base non-specific and adenylic acid preferential ribonuclease from the fruit bodies of *Lentinus edodes*. *Bioscience, Biotechnology, and Biochemistry*, 56, 2003–2010.

Krautz, R., Arefin, B. & Theopold, U. (2014) Damage signals in the insect immune response. *Frontiers in Plant Science*, 5, 103421.

Kurihara, H., Mitsui, Y., Ohgi, K., Irie, M., Mizuno, H. & Nakamura, K.T. (1992) Crystal and molecular structure of RNase Rh, a new class of microbial ribonuclease from *Rhizopus niveus*. *FEBS Letters*, 306, 189–192.

Liu, S. & Bonning, B.C. (2019) The principal salivary gland is the primary source of digestive enzymes in the saliva of the brown marmorated stink bug, *Halyomorpha halys*. *Frontiers in Physiology*, 10, 492476.

Liu, S., Lomate, P.R. & Bonning, B.C. (2018) Tissue-specific transcription of proteases and nucleases across the accessory salivary gland, principal salivary gland and gut of *Nezara viridula*. *Insect Biochemistry and Molecular Biology*, 103, 36–45.

Luhtala, N. & Parker, R. (2010) T2 family ribonucleases: ancient enzymes with diverse roles. *Trends in Biochemical Sciences*, 35, 253–259.

Luo, T., Yang, H., Li, F., Zhang, X. & Xu, X. (2006) Purification, characterization and cDNA cloning of a novel lipopolysaccharide-binding lectin from the shrimp *Penaeus monodon*. *Developmental and Comparative Immunology*, 30, 607–617.

MacIntosh, G.C. (2011) RNase T2 family: enzymatic properties, functional diversity, and evolution of ancient ribonucleases. In A. Nicholson (Eds.) *Ribonucleases Nucleic Acids and Molecular Biology*. Springer.

MacIntosh, G.C., Bariola, P.A., Newbigin, E. & Green, P.J. (2001) Characterization of Rny1, the *Saccharomyces cerevisiae* member of the T2 RNase family of RNases: unexpected functions for ancient enzymes? *Proceedings of the National Academy of Sciences*, 98, 1018–1023.

Mannucci, A., Panariello, L., Abenaim, L., Coltelli, M.B., Ranieri, A., Conti, B. et al. (2024) From food waste to functional biopolymers: characterization of chitin and chitosan produced from prepupae of black soldier fly reared with different food waste-based diets. *Foods*, 13, 278.

McClure, B.A., Haring, V., Ebert, P.R., Anderson, M.A., Simpson, R.J., Sakiyama, F. et al. (1989) Style self-incompatibility gene products of *Nicotlana alata* are ribonucleases. *Nature*, 342, 955–957.

Möller, S., Croning, M.D.R. & Apweiler, R. (2001) Evaluation of methods for the prediction of membrane spanning regions. *Bioinformatics*, 17, 646–653.

Moretta, A., Salvia, R., Scieuzo, C., Di Somma, A., Vogel, H., Pucci, P. et al. (2020) A bioinformatic study of antimicrobial peptides identified in the Black Soldier Fly (BSF) *Hermetia illucens* (Diptera: Stratiomyidae). *Scientific Reports*, 10, 16875.

Nicholson, A.W. (2011) Ribonuclease III and the role of double-stranded RNA processing in bacterial systems. In A. Nicholson (Eds.) *Ribonucleases Nucleic Acids and Molecular Biology*. Springer.

Parisi, M.G., Baranzini, N., Dara, M., La Corte, C., Vizioli, J. & Cammarata, M. (2022) AIF-1 and RNASET2 are involved in the inflammatory response in the Mediterranean mussel *Mytilus galloprovincialis* following Vibrio infection. *Fish & Shellfish Immunology*, 127, 109–118.

Pimentel, A.C., Montali, A., Bruno, D. & Tettamanti, G. (2017) Metabolic adjustment of the larval fat body in *Hermetia illucens* to dietary conditions. *Journal of Asia-Pacific Entomology*, 20, 1307–1313.

Pizzo, E. & D'Alessio, G. (2007) The success of the RNase scaffold in the advance of biosciences and in evolution. *Gene*, 406, 8–12.

Rose, A., Chiu, Y.C., Showman, C., Ku, K.M., Jaczynski, J. & Matak, K. (2023) Characterization of protein concentrates obtained by defatting cricket, locust, and silkworm powders using one-step organic solvent extraction. *LWT*, 182, 114876.

Sato, K. & Egami, F. (1957) Studies on ribonucleases in takadiastase. I. *The Journal of Biochemistry*, 44, 753–767.

Scieuzo, C., Giglio, F., Rinaldi, R., Lekka, M.E., Cozzolino, F., Monaco, V. et al. (2023) *In vitro* evaluation of the antibacterial activity of the peptide fractions extracted from the hemolymph of *Hermetia illucens* (Diptera: Stratiomyidae). *Insects*, 14, 464.

Sievers, F., Wilm, A., Dineen, D., Gibson, T.J., Karplus, K., Li, W. et al. (2011) Fast, scalable generation of high-quality protein multiple sequence alignments using Clustal Omega. *Molecular Systems Biology*, 7, 539.

Tettamanti, G. & Bruno, D. (2024) Black soldier fly larvae should be considered beyond their use as feedstuff. *Journal of Insects as Food and Feed*, 10, 1–7.

Tettamanti, G., Grimaldi, A., Ferrarese, R., Palazzi, M., Perletti, G., Valvassori, R. et al. (2003) Leech responses to tissue transplantation. *Tissue and Cell*, 35, 199–212.

Tettamanti, G., Grimaldi, A., Valvassori, R., Rinaldi, L. & de Eguileor, M. (2003) Vascular endothelial growth factor is involved in neoangiogenesis in *Hirudo medicinalis* (Annelida, Hirudinea). *Cytokine*, 22, 168–179.

Teufel, F., Almagro Armenteros, J.J., Johansen, A.R., Gíslason, M.H., Pihl, S.I., Tsirigos, K.D. et al. (2022) SignalP 6.0 predicts all five types of signal peptides using protein language models. *Nature Biotechnology*, 40, 1023–1025.

Torrent, M., Andreu, D., Nogués, V.M. & Boix, E. (2011) Connecting peptide physicochemical and antimicrobial properties by a rational prediction model. *PLoS One*, 6, e16968.

Torrent, M., Sánchez, D., Buzón, V., Nogués, M.V., Cladera, J. & Boix, E. (2009) Comparison of the membrane interaction mechanism of two antimicrobial RNases: RNase 3/ECP and RNase 7. *Biochimica et Biophysica Acta (BBA) - Biomembranes*, 1788, 1116–1125.

Torrent, M., Di Tommaso, P., Pulido, D., Nogués, M.V., Notredame, C., Boix, E. et al. (2012) AMPA: an automated web server for prediction of protein antimicrobial regions. *Bioinformatics*, 28, 130–131.

Torrent, M., de laTorre, B.G., Nogués, V.M., Andreu, D. & Boix, E. (2009) Bactericidal and membrane disruption activities of the eosinophil cationic protein are largely retained in an N-terminal fragment. *Biochemical Journal*, 421, 425–434.
Vogel, H., Müller, A., Heckel, D.G., Gutzeit, H. & Vilcinskas, A. (2018) Nutritional immunology: diversification and diet-dependent expression of antimicrobial peptides in the black soldier fly *Hermetia illucens*. *Developmental and Comparative Immunology*, 78, 141–148.
Waterhouse, A.M., Procter, J.B., Martin, D.M.A., Clamp, M. & Barton, G.J. (2009) Jalview version 2—a multiple sequence alignment editor and analysis workbench. *Bioinformatics*, 25, 1189–1191.
Yeaman, M.R. & Yount, N.Y. (2003) Mechanisms of antimicrobial peptide action and resistance. *Pharmacological Reviews*, 55, 27–55.
Yu, S.-J., Liao, E.-C., Sheu, M.-L., Chang, D.-T.M. & Tsai, J.-J. (2015) Cell-penetrating peptide derived from human eosinophil cationic protein inhibits mite allergen Der p 2 induced inflammasome activation. *PLoS One*, 10, e0121393.
Yu, X.Q. & Kanost, M.R. (2000) Immulectin-2, a lipopolysaccharide-specific lectin from an insect, *Manduca sexta*, is induced in response to gram-negative bacteria. *Journal of Biological Chemistry*, 275, 37373–37381.
Yue, Y., Deng, J., Wang, H., Lv, T., Dou, W., Jiao, Y. et al. (2023) Two secretory T2 RNases act as cytotoxic factors contributing to the virulence of an insect fungal pathogen. *Journal of Agricultural and Food Chemistry*, 71, 7069–7081.
Zdybicka-Barabas, A., Bulak, P., Polakowski, C., Bieganowski, A., Waśko, A. & Cytryńska, M. (2017) Immune response in the larvae of the black soldier fly *Hermetia illucens*. *Invertebrate Survival Journal*, 14, 9–17.
Zhang, Y. (2008) I-TASSER server for protein 3D structure prediction. *BMC Bioinformatics*, 9, 40.
Zhou, L., Meng, G., Zhu, L., Ma, L. & Chen, K. (2024) Insect antimicrobial peptides as guardians of immunity and beyond: a review. *International Journal of Molecular Sciences*, 25, 3835.

SUPPORTING INFORMATION

Additional supporting information can be found online in the Supporting Information section at the end of this article.

How to cite this article: Caramella, S., Baranzini, N., Bruno, D., Orlandi, V. T., Mohamed, A., Bolognese, F. et al. (2024) Exploring the role of RNASET2 in the immune response of black soldier fly larvae. *Archives of Insect Biochemistry and Physiology*, 116, e22146. https://doi.org/10.1002/arch.22146